

NOAA Technical Memorandum ERL PMEL-61

SEDIMENTATION RATES IN PUGET SOUND FROM  $^{210}\text{PB}$  MEASUREMENTS

J. W. Lavelle  
G. J. Massoth

E. A. Crecelius  
Battelle Marine Research Laboratory  
Sequim, Washington

Pacific Marine Environmental Laboratory  
Seattle, Washington  
January 1985



UNITED STATES  
DEPARTMENT OF COMMERCE

Malcolm Baldrige,  
Secretary

NATIONAL OCEANIC AND  
ATMOSPHERIC ADMINISTRATION

Environmental Research  
Laboratories

Vernon E. Derr,  
Director

**NOTICE**

**Mention of a commercial company or product does not constitute an endorsement by NOAA/ERL. Use of information from this publication concerning proprietary products or the tests of such products for publicity or advertising purposes is not authorized.**

---

**Contribution No. 732 from NOAA/Pacific Marine Environmental Laboratory**

## CONTENTS

	<u>Page</u>
ABSTRACT.....	1
1. INTRODUCTION.....	1
2. DATA ACQUISITION AND ANALYSIS.....	3
3. RESULTS AND DISCUSSION.....	6
4. CONCLUSIONS.....	19
5. ACKNOWLEDGMENTS.....	20
6. REFERENCES.....	21
Appendix I: Salt Correction Calculations.....	24
Appendix II: Data Tables.....	26



## Sedimentation Rates in Puget Sound from $^{210}\text{Pb}$ Measurements

J. W. Lavelle  
G. J. Massoth  
E. A. Crecelius\*

**ABSTRACT.** Sixteen  $^{210}\text{Pb}$  profiles from sites along the axis of the Main Basin of Puget Sound show that bottom sediments are accumulating at rates of 0.26 to 1.20 g/cm<sup>2</sup>/yr; these along with seven rates earlier published suggest highest accumulation nearly midway along the length of this tidal current-dominated basin. Bioturbated surface layers of cores have also been found to be as deep as 40 cm, but biologic mixing rates are poorly determined. Individual  $^{210}\text{Pb}$  accumulation rates have a range of from approximately one to five times areal average accumulation rates based on estimates of recent sediment input from riverine and shoreline sources.

### 1. INTRODUCTION

Puget Sound, sculpted by glacial advance and retreat, is the deepest estuarine system in the contiguous United States. Its Main Basin, with relatively steep side walls, is presently more than 200 m deep, though at the time of the last glaciation that depth extended to more than 600 m. The sedimentation that has occurred since the last glacial retreat continues with sediments provided by rivers, shoreline erosion, and possibly submarine sources. It is of particular interest today because it is one important way by which anthropogenic particulate-borne contaminants are eventually isolated from the marine biosphere. This report focuses on the rate of recent sedimentation and its pattern along the axis of the Main Basin of Puget Sound.

$^{210}\text{Pb}$  has seen considerable geophysical use in determining sedimentation rates (e.g. Robbins, 1978).  $^{210}\text{Pb}$  is a useful isotope because it is naturally and constantly produced, attaches readily and nearly irreversibly to particles, and has a half-life of 22.3 years that allows study of sedimentation over approximately the last 70 years. Estimates of sedimentation rates come from analysis of profiles of the concentration of the isotope in sediment cores.

Puget Sound can be divided into several regions: North Sound, Whidbey Basin, Central Sound (Main Basin), South Sound, and Hood Canal (e.g. Downing, 1983). The Main Basin is defined as the area south of the sill at Admiralty Inlet and north of the sill at Tacoma Narrows (Fig. 1). Our data and discussions concern Main Basin sedimentation. Others have also reported on  $^{210}\text{Pb}$  determinations of sedimentation rates in the Puget Sound region (Blank, 1950; Shell, 1974; Shell and Nevissi, 1977; Shell *et al.* 1977; Link, 1982) but nearly all of the cores except those reported by Carpenter *et al.* (1985) were

---

\*Battelle Marine Research Laboratory, Sequim, WA 98382

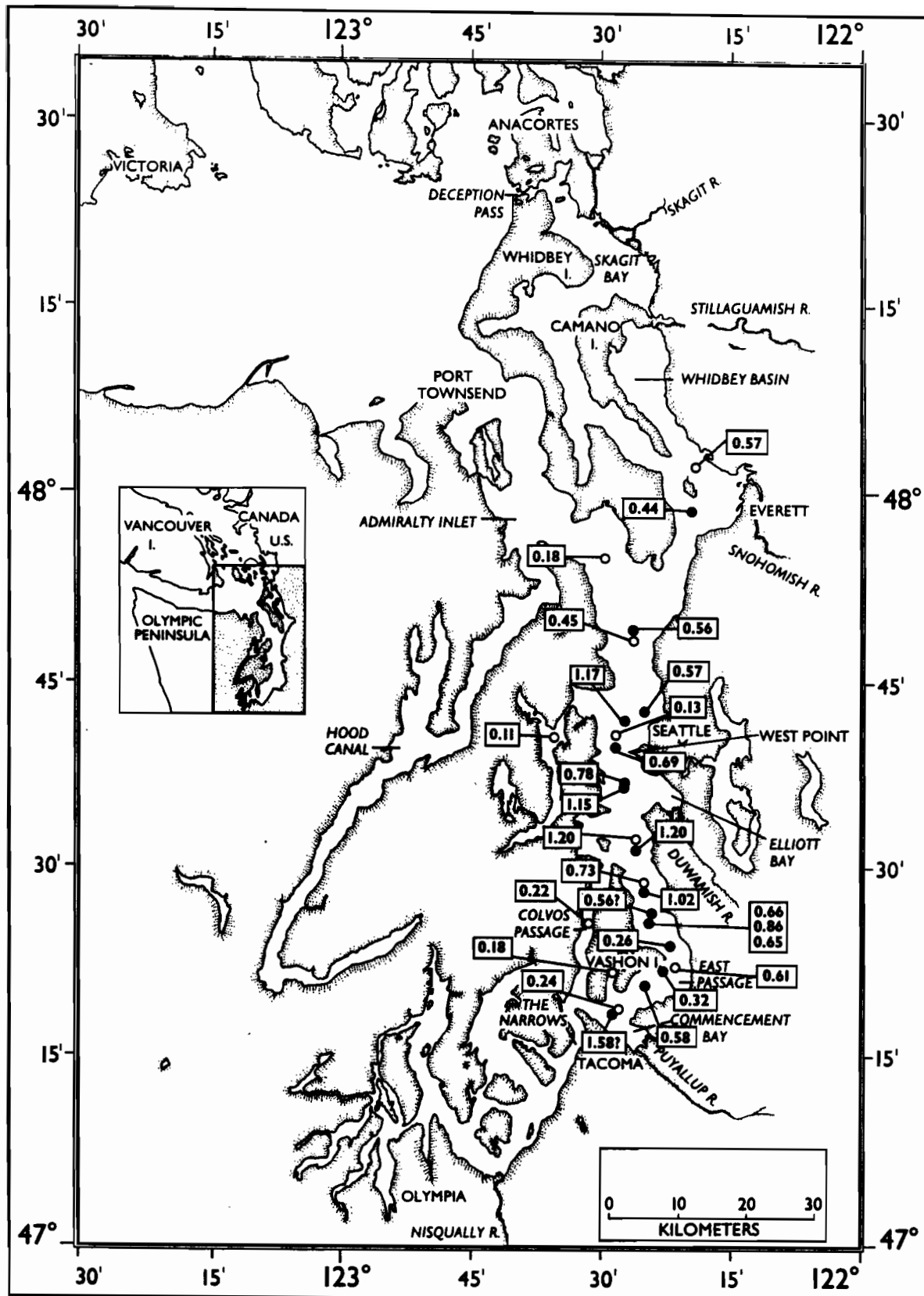


Fig. 1.--Stations locations and inferred sediment accumulation rates (g/cm<sup>2</sup>/yr). Closed circles are from our analyses and the open circles from Carpenter *et al.* (1985).

taken with coring devices which are known to shorten or compress cores. Our cores were taken with a corer that minimizes distortion and provides data to greater depth than most cores previously taken. These results, when added to those of Carpenter *et al.* (1985), also more than double the number of stations along the axis of the Main Basin. As a consequence, a better definition of sedimentation patterns is possible leading to a somewhat different conclusion than that previously drawn.

## 2. DATA ACQUISITION AND ANALYSIS

Cores along the axis of the Main Basin were taken at seven stations (Cores 11-17, Table 1) in August, 1982, and at 9 stations (Cores 1-9, Table 1) in March, 1984 (Fig. 1). A single additional core was taken in Whidbey Basin (Core #10). The samples were taken with a Kasten corer (3.0 × 0.15 × 0.15 m), a device that minimizes the core shortening effects of conventional gravity corers (Lebel *et al.*, 1982) and also provides much longer cores than normally collected by box corer. Core length varied from 230 to 300 m, considerably longer than most cores previously reported for Puget Sound.

Sections 2 cm (1984 cores) or 5 cm (1982 cores) thick were removed at a number ( $11 \leq n \leq 20$ ) of depths in the core and homogenized. Homogenization precludes observations of high wave-number variations in  $^{210}\text{Pb}$  activity as observed by Carpenter *et al.* (1985), but a consequent effect on accumulation rate estimates should not be expected.  $^{210}\text{Pb}$  analysis on sections was conducted using  $\alpha$  ( $^{210}\text{Po}$  granddaughter) spectrometry. Each section was also analyzed for water content, and a salt corrected porosity,  $\phi$ , and a  $^{210}\text{Pb}$  activity per unit mass of salt-free sediment was determined. Appendix I details the salt correction calculation.

Unsupported  $^{210}\text{Pb}$  activity was calculated from total  $^{210}\text{Pb}$  activity by subtracting the background activity calculated from the samples deep in the core which indicated a constant activity had been reached. In a few cores (Cores #6, 13, 14, 15) this was not possible and a nominal value of 1 dpm/g for background was used, and the sensitivity of results to that choice was examined.

The resulting profiles of unsupported  $^{210}\text{Pb}$  activity (Figs. 2a-i) showed considerable differences in slope at depth (proportional to sedimentation velocity) and in the thickness of the bioturbated surface layer. Except for the upper one or two samples in each core, the associated porosity data was relatively constant with depth. A mean porosity below the bioturbated layer for each core (Table 1) was calculated and used in the subsequent analyses.

The profiles were evaluated with a steady two-layer advection-diffusion model (e.g. Goldberg and Koide, 1962; Robbins, 1978):

$$w_s \frac{\partial C}{\partial z} - \frac{\partial}{\partial z} (A \frac{\partial C}{\partial z}) = -\lambda C \quad (1)$$

where  $C$  is the unsupported  $^{210}\text{Pb}$  activity,  $z$  the vertical coordinate (positive downward),  $w_s$  a constant sedimentation velocity,  $A$  the mixing coefficient due to bioturbation (or biodiffusivity) and  $\lambda$  ( $= 0.03114 \text{ yr}^{-1}$ ) the radioisotope decay constant. The generalization of (1) for non-constant porosity is given

Table 1:--Station data and best-fit model results. Accumulation rates are calculated using Eq. 2 with  $\rho = 2.6 \text{ gm/cm}^3$ , a value measured on representative samples; mean porosity is based on samples below the bioturbation depth. A supported  $^{210}\text{Pb}$  activity of 1.0 dmp/g is a nominal value. Confidence limits are at the 95% level.

Core No.	Latitude (N)/ Latitude (W)	Water Depth (m)	Supported $^{210}\text{Pb}$ Activity (dpm/g)	Number of Samples*	Bioturbation Depth (cm)	Mixing Coefficient ( $\text{cm}^2/\text{yr}$ )	$^{210}\text{Pb}$ Surface Concentration (dpm/g)	Sedimentation Velocity ( $\text{cm}/\text{yr}$ )	Mean Porosity	Accumulation Rate ( $\text{gm}/\text{cm}^2/\text{yr}$ )
1	47°21.9'/122°22.0'	178	0.72	11	15	30	8.0	0.73±0.05	0.832±0.008	0.32±0.04
2	47°23.8'/122°21.2'	207	0.72	12	30	30	9.6	0.53±0.04	0.809±0.010	0.26±0.03
3	47°25.6'/122°23.5'	193	0.94	17	35	300	9.1	1.43±0.07	0.822±0.008	0.66±0.06
4	47°25.6'/122°23.5'	193	0.97	17	20	30	10.3	1.90±0.12	0.825±0.006	0.86±0.08
5	47°25.6'/122°23.5'	193	0.82	18	40	30	9.7	1.43±0.08	0.825±0.007	0.65±0.06
6	47°31.6'/122°25.4'	201	1.0	19	35	300	10.7	2.48±0.23	0.814±0.007	1.20±0.16
6a	-	-	0.5	19	35	300	10.6	3.12±0.18	0.814±0.007	1.51±0.14
7	47°36.9'/122°26.75'	205	1.1	17	15	30	11.7	1.52±0.07	0.803±0.008	0.78±0.07
8	47°39.75'/122°27.9'	229	0.87	16	30	30	11.9	1.20±0.08	0.779±0.008	0.69±0.07
9	47°26.7'/122°23.55'	238	0.54	11	10	30	5.2	0.66±0.09	0.672±0.037	0.56±0.14
10	47°58.8'/122°19.5'	159	0.60	13	5	30	8.4	0.86±0.09	0.805±0.006	0.44±0.06
11	47°49.4'/122°25.8'	173	1.01	8	10	30	11.1	0.64±0.06	0.665±0.017	0.56±0.08
12	47°43.0'/122°24.3'	188	0.81	13	35	270	10.6	0.98±0.04	0.777±0.008	0.57±0.04
12a	-	-	0.81	13	35	1000	10.2	0.97±0.05	0.777±0.008	0.56±0.05
12b	-	-	0.81	13	35	30	13.5	1.03±0.07	0.777±0.008	0.60±0.06
13	47°42.3'/122°26.4'	199	1.0	14	35	30	12.5	1.92±0.09	0.765±0.006	1.17±0.08
13a	-	-	1.0	14	35	70	11.5	1.88±0.09	0.765±0.006	1.15±0.08
13b	-	-	0.5	14	35	30	11.4	2.37±0.14	0.765±0.006	1.45±0.11
14	47°36.9'/122°26.8'	205	1.0	9	35	30	13.8	2.14±0.09	0.794±0.009	1.15±0.10
14a	-	-	0.5	9	35	30	13.4	2.66±0.14	0.794±0.009	1.42±0.14
15	47°28.8'/122°24.4'	197	1.0	10	35	30	12.3	2.21±0.08	0.822±0.011	1.02±0.10
15a	-	-	1.0	10	35	70	11.3	2.17±0.09	0.822±0.011	1.00±0.10
15b	-	-	0.5	10	35	30	12.3	2.68±0.14	0.822±0.011	1.24±0.14
16	47°21.0'/122°24.4'	185	1.34	8	10	30	9.5	1.21±0.14	0.815±0.012	0.58±0.10
17	47°18.7'/122°27.7'	183	0.62	8	10	30	3.7	1.81±0.17	0.665±0.026	1.58±0.27

\*Supported  $^{210}\text{Pb}$  activity



by Aller *et al.* (1979) and Berner (1980). The mass accumulation rate  $r$ , and sedimentation velocity are related:

$$r = \rho_s (1-\phi) w_s \quad (2)$$

where  $\rho_s$  is the dry sediment density and  $\phi$  is the porosity. Mixing by resuspension has not been considered because the resuspension thickness in the Main Basin is only on the order of 1 mm (Lavelle *et al.* 1984). Boundary conditions imposed on the solution of (1) are that the activity flux of the surface equals  $w_s C_0$  and activity at depth is zero.

The diffusion coefficient,  $A$ , was taken to be discontinuous having a constant value ( $A_1$ ) in an upper bioturbated layer (thickness  $h$ ) and a negligible value below ( $A_2 = 0$ ; e.g. Robbins, 1978). This recognizes the fact that a sediment column can have a rapidly mixed surface layer (or layers) where biota are active that overlies a region where mixing is slow or nil (e.g. Robbins and Edgington, 1975). Other diffusivity profiles to simulate the role and distribution of infauna mixing the sediment have been recently suggested (e.g. Peng *et al.*, 1979; Christensen, 1982), but it can be shown (by inserting an exponential form for  $C$  in (1) and requiring the solution to the resulting equation for diffusivity ( $A_2$ ) not increase with depth) that data having an exponential  $z$ -dependence in the second layer (as does this data) can only support a constant biodiffusivity in that layer. Further that constant must take a small value ( $A_2 \sim 0$ ) because deep in the core little bioturbation could be expected. Though the transition from the upper layer mixing rate ( $A_1$ ) to a negligible rate ( $A_2 \sim 0$ ) must actually occur over a finite interval, our data cannot resolve the apparent rapid transition from one region to another.

When  $A$  takes constant values  $A_1$  and  $A_2$  in the upper and lower layers respectively, the solution of (1) in steady state subject to a flux ( $=w_s C_0$ ) condition at the surface, zero concentration at depth, and matching concentration and flux at the layer interface depth,  $h$ , is:

$$\begin{aligned} C_1 &= a_1 e^{(\beta_1 + \gamma_1)z} + a_2 e^{(\beta_1 - \gamma_1)z} & 0 < z < h \\ C_2 &= a_3 e^{(\beta_2 - \gamma_2)z} & z < h \end{aligned} \quad (3)$$

where:

$$\begin{aligned} a_1 &= \{-2\beta_1 C_0 (\gamma_2\beta_1 - \gamma_1\beta_2)e^{-\gamma_1 h}\}/D \\ a_2 &= \{2\beta_1 C_0 (\gamma_2\beta_1 + \gamma_1\beta_2)e^{+\gamma_1 h}\}/D \\ a_3 &= \{4\beta_1 \beta_2 \gamma_1 C_0 e^{-(\beta_2 - \beta_1 - \gamma_2)h}\}/D \\ D &= [(\beta_1 + \gamma_1) (\gamma_2\beta_1 + \gamma_1\beta_2)]e^{\gamma_1 h} - [(\beta_1 - \gamma_1) (\gamma_2\beta_1 - \gamma_1\beta_2)]e^{-\gamma_1 h} \end{aligned}$$

Here  $\beta_i = (w_s/2A_i)$  and  $\gamma_i = (\beta_i^2 + \lambda/A_i)^{1/2}$ , and the flux to the sediment surface is  $w_s C_0$ .

Eq. 3 shows that profiles are exponential in depth in the second layer but the exponential decay length scale (i.e.  $(\beta_2 - \gamma_2)^{-1}$ ) depends on both  $w_s$  and  $A_2$ . Thus, neither can be uniquely determined by a single tracer profile of

data in the second layer though both parameters have limited ranges of values because both must be positive numbers. When  $(\beta_2 - \gamma_2)^{-1} = k$  and  $k$  is large, this equation can be used to show that small changes in  $A_2$  away from zero strongly affect the inferred  $w_s$  as Carpenter *et al.*, (1982) numerically found. At smaller  $k$  values (as in our cases), a small non-zero  $A_2$  has much less effect on the inferred  $w_s$ . Consequently, for our analyses,  $A_2$  was set to zero (e.g., as in Guinasso and Shink, 1975; Carpenter *et al.*, 1985).

Values for the bioturbated layer depth,  $h$ , were determined by noting for each profile the approximate depth at which the exponential depth dependence of  $^{210}\text{Pb}$  activity began (Fig. 2). Values for  $h$  ranged from 5 to 40 cm, a larger range than that determined by Carpenter *et al.* (1985) (4 to 18 cm) for Main Basin cores.

Least-squares fitting of several profiles for  $A_1$ ,  $C_0$  (surface activity), and  $w_s$  indicated that these profiles poorly determine the value of  $A_1$  (contrast Carpenter *et al.*, 1985). This result is alternatively seen in a comparison of profiles for several  $A_1$  values in Fig. 3 (as in Robbins (1978) and Peng *et al.* (1979)). For core #12, for example, differences in profiles for  $A_1 = 30$  and 270  $\text{cm}^2/\text{yr}$  are slight; a profile for  $A_1 = 1000 \text{ cm}^2/\text{yr}$  was indistinguishable from the 270  $\text{cm}^2/\text{yr}$  profile. On the other hand, values much smaller than 30  $\text{cm}^2/\text{yr}$  are not warranted by the data. In light of this, for most profiles  $A_1$  was given a value of 30  $\text{cm}^2/\text{yr}$ , near the value (34.7  $\text{cm}^2/\text{yr}$ ) determined by  $^{234}\text{Th}$  analysis on Core #16 by J. Murray (personal communication, 1984). In a few cases (e.g. Core #12, Fig. 3) a larger value of  $A_1$  gave a slightly better fit. Finally, the values of  $w_s$  are not very sensitive to the values given  $A_1$  (compare results for samples:  $s$  (12, 12a, 12b); (13, 13a); (15, 15a) in Table 1) so uncertainty in  $A_1$  does not impede the deposition rate analysis. The values of  $w_s$  and  $C_0$  were determined by fitting the two layer solution of (1) to the data and a value for  $r$  for each profile was then calculated (2).

The sensitivity of the inferred sedimentation velocity to the value of the supported  $^{210}\text{Pb}$  activity was investigated for Cores #6, 13, 14, 15 which had been given a nominal background of 1 dpm/g. This was done by reassigning a value of 0.5 dpm/g to the background activity. A comparison of best-fit results for both values of background (Table 1: (6, 6a); (13, 13b); (14, 14a), (15, 15b)) show an increase of  $w_s$  of approximately 25% for each core when the smaller background activity is used.

Sedimentation velocities were converted to mass accumulation rates (Table 1) using mean porosity values as described earlier and a value measured on representative samples of 2.6  $\text{g}/\text{cm}^3$  for  $\rho_s$ . Confidence limits in Table 1 are at the 95% level and were calculated for these non-linear fits in the manner of Jenkins and Watts (1968).

### 3. RESULTS AND DISCUSSION

Accumulation rates determined in this way range from 0.26 to 1.20  $\text{gm}/\text{cm}^2/\text{yr}$  (Fig. 1); the rates for axial stations of Carpenter *et al.* (1985) range from 0.18 to 1.20  $\text{gm}/\text{cm}^2/\text{yr}$  (Fig. 1). Rates for Cores #9 and 17 are suspect because of the erratic pattern seen in both porosity and  $^{210}\text{Pb}$

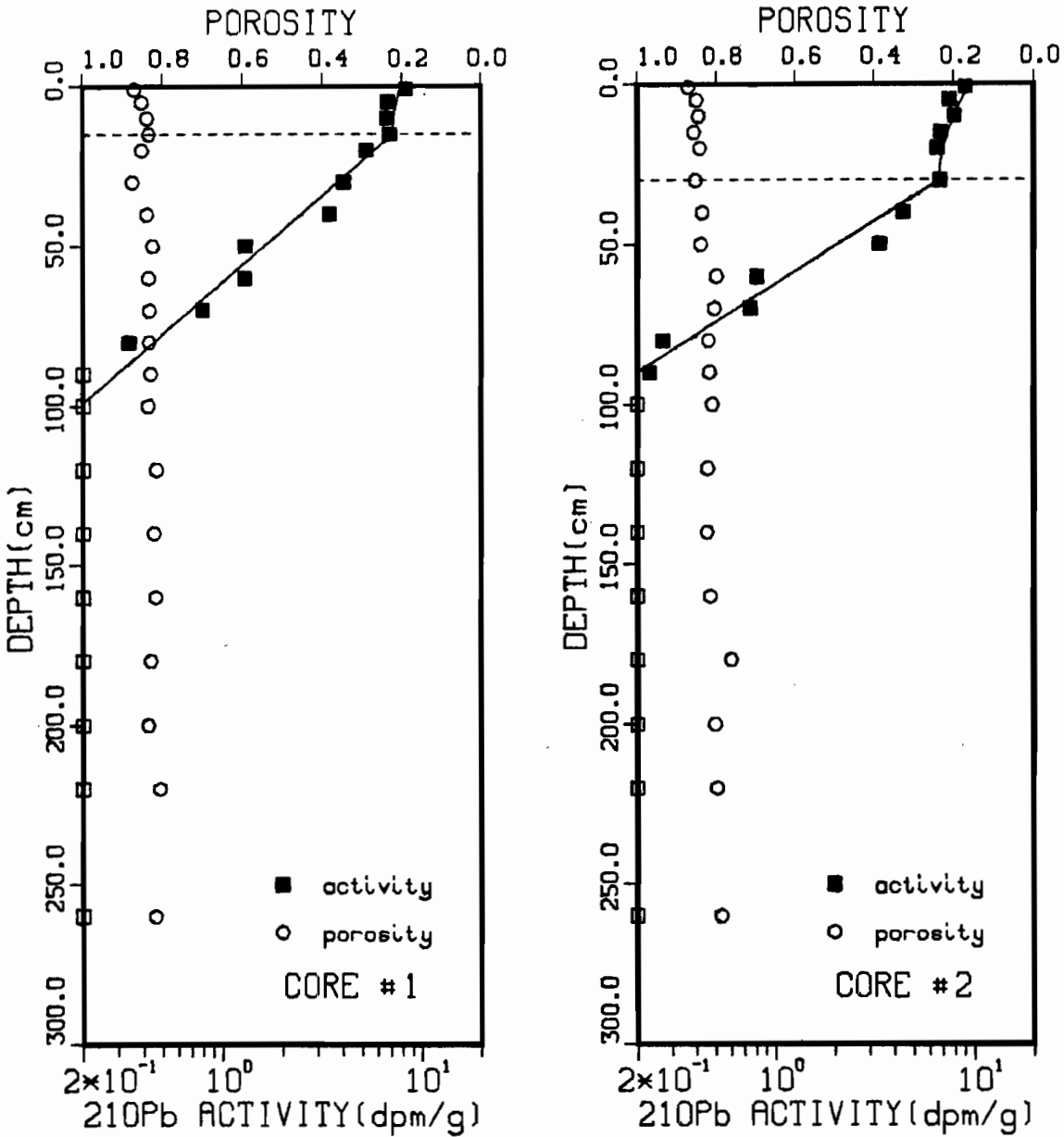


Fig. 2a.--Profiles of unsupported  $^{210}\text{Pb}$  activity and porosity as a function of depth.  $^{210}\text{Pb}$  activities represented by solid boxes were used in determining best-fit parameter values. Samples with no unsupported  $^{210}\text{Pb}$  activity (total activity at background) fall along the ordinate axis. Porosity values are given by circles. The horizontal dashed line marks the boundary between the bioturbated layer and the region below.

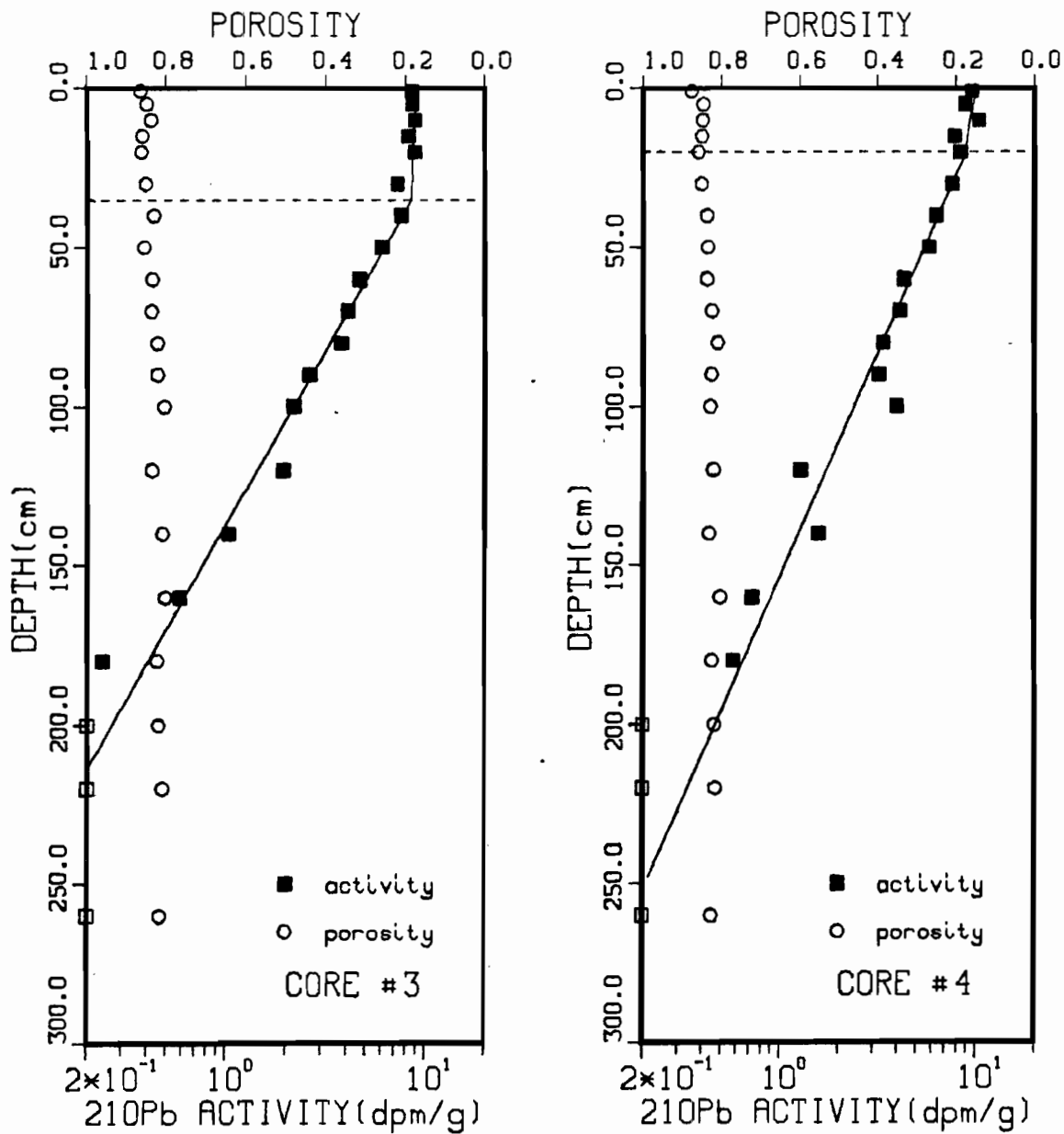


Fig. 2b.--Profiles of unsupported  $^{210}\text{Pb}$  activity and porosity as a function of depth.  $^{210}\text{Pb}$  activities represented by solid boxes were used in determining best-fit parameter values. Samples with no unsupported  $^{210}\text{Pb}$  activity (total activity at background) fall along the ordinate axis. Porosity values are given by circles. The horizontal dashed line marks the boundary between the bioturbated layer and the region below.

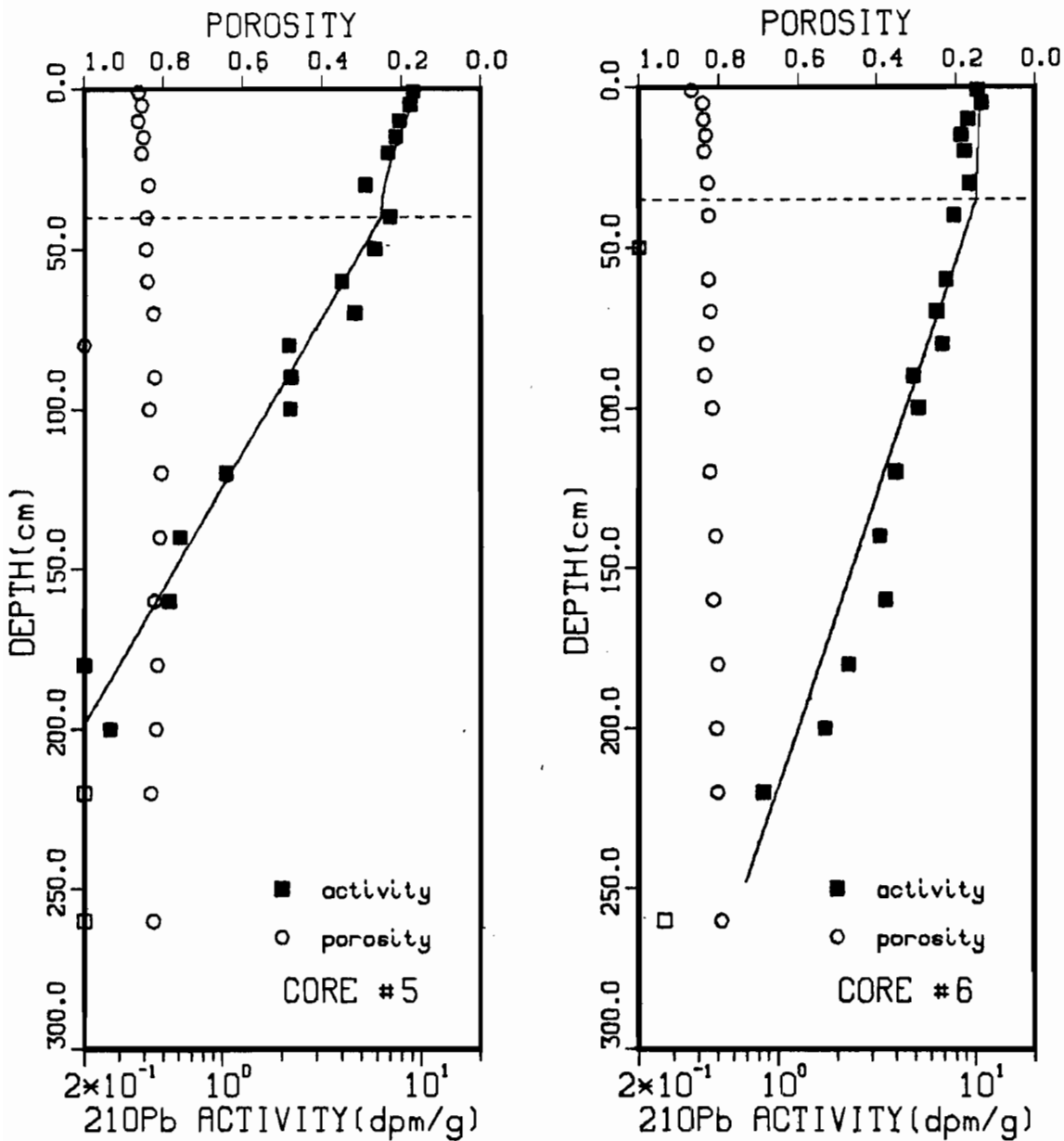


Fig. 2c.--Profiles of unsupported <sup>210</sup>Pb activity and porosity as a function of depth. <sup>210</sup>Pb activities represented by solid boxes were used in determining best-fit parameter values. Samples with no unsupported <sup>210</sup>Pb activity (total activity at background) fall along the ordinate axis. Porosity values are given by circles. The horizontal dashed line marks the boundary between the bioturbated layer and the region below.

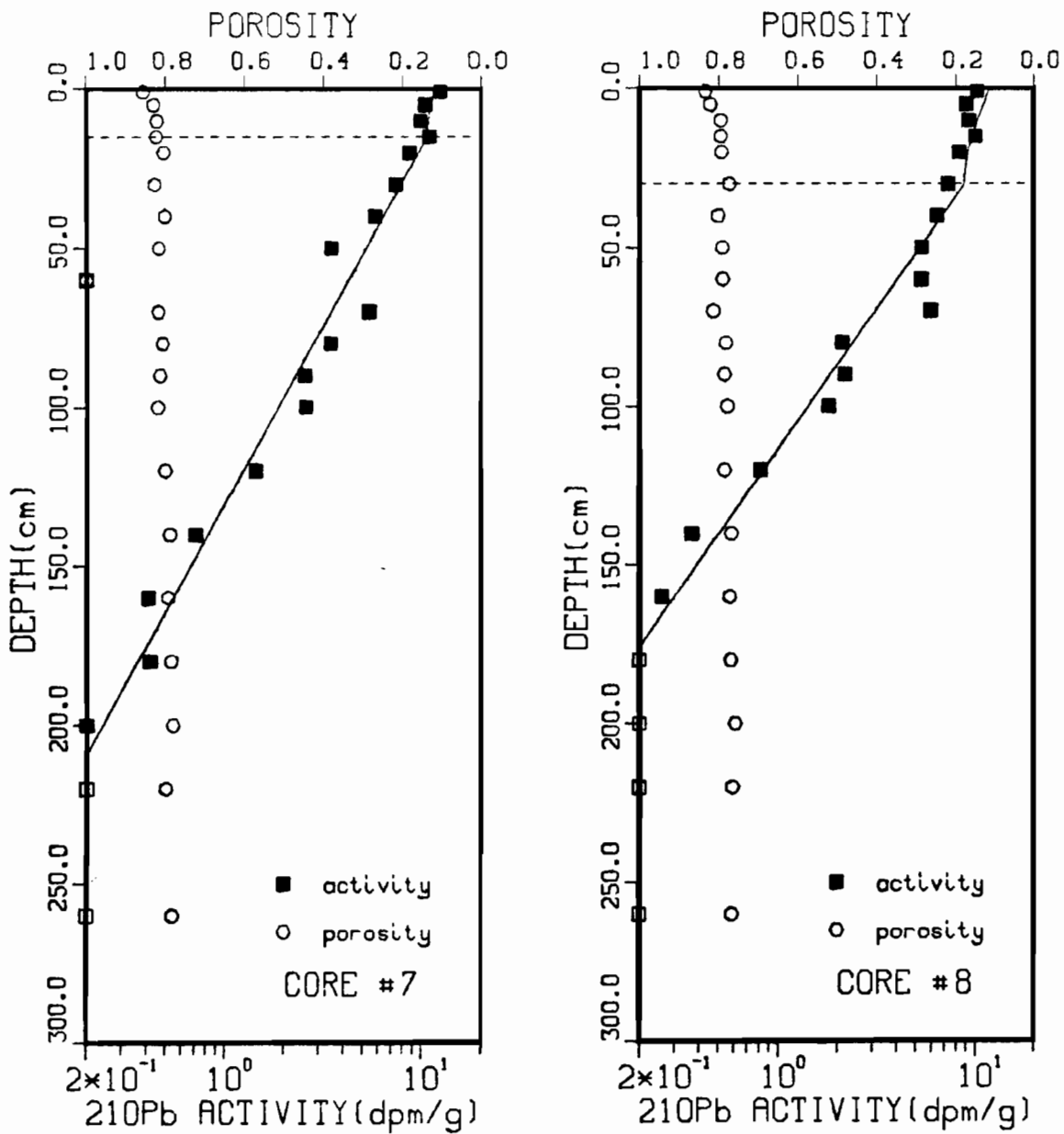


Fig. 2d.--Profiles of unsupported  $^{210}\text{Pb}$  activity and porosity as a function of depth.  $^{210}\text{Pb}$  activities represented by solid boxes were used in determining best-fit parameter values. Samples with no unsupported  $^{210}\text{Pb}$  activity (total activity at background) fall along the ordinate axis. Porosity values are given by circles. The horizontal dashed line marks the boundary between the bioturbated layer and the region below.

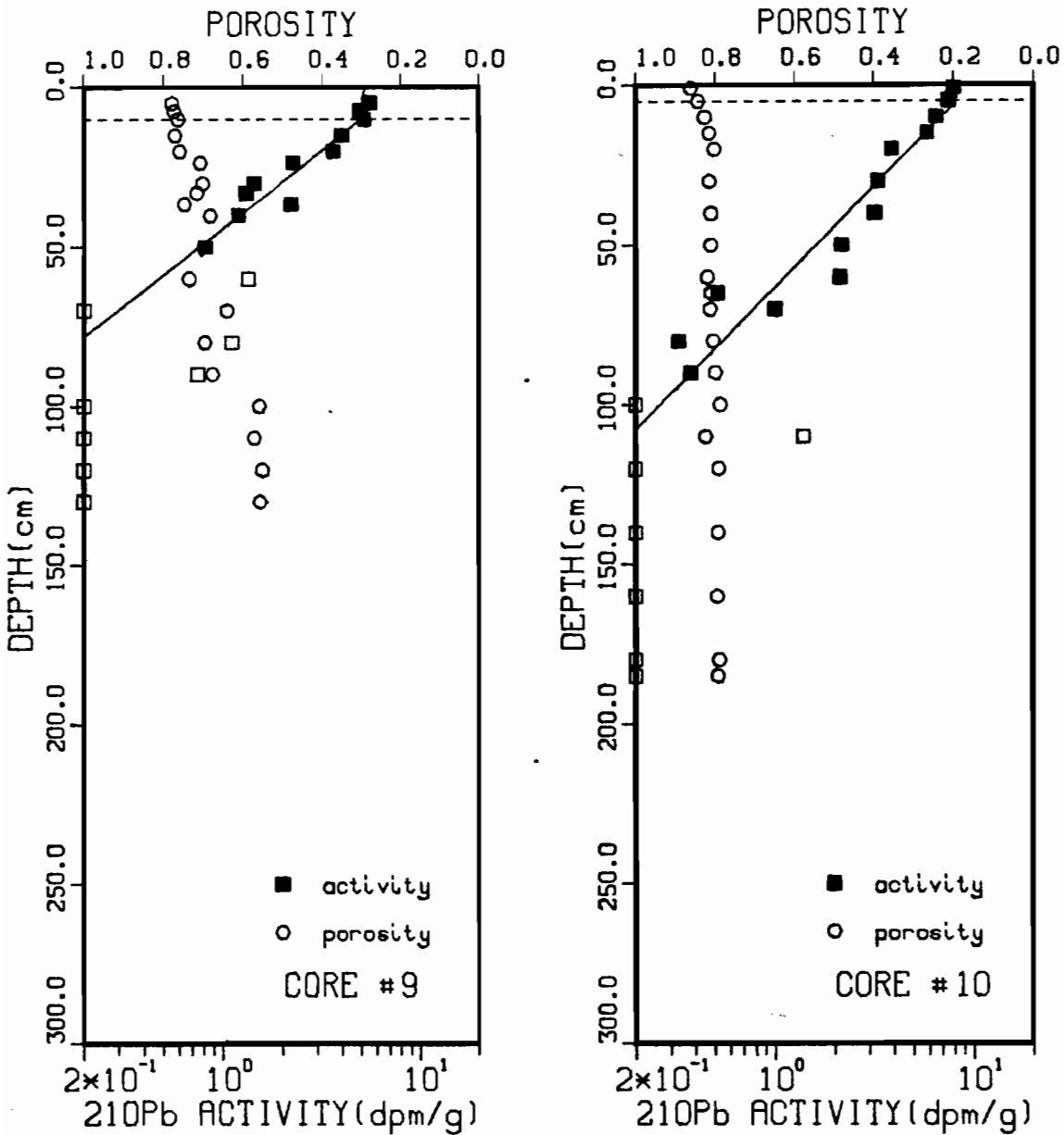


Fig. 2e.--Profiles of unsupported  $^{210}\text{Pb}$  activity and porosity as a function of depth.  $^{210}\text{Pb}$  activities represented by solid boxes were used in determining best-fit parameter values. Samples with no unsupported  $^{210}\text{Pb}$  activity (total activity at background) fall along the ordinate axis. Porosity values are given by circles. The horizontal dashed line marks the boundary between the bioturbated layer and the region below.

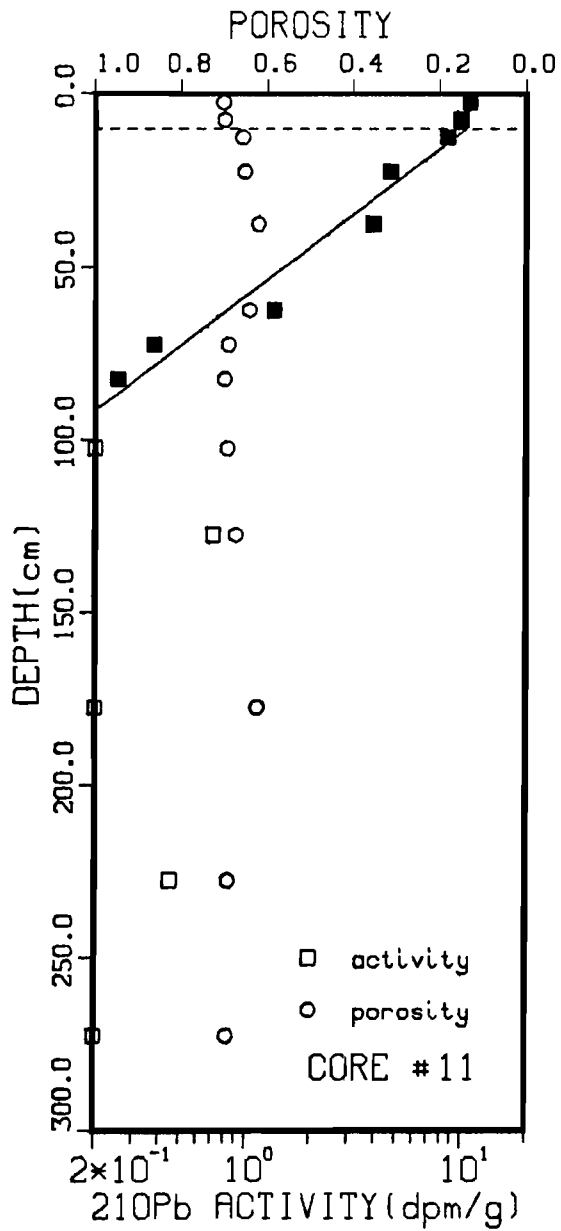


Fig. 2f.--Profile of unsupported  $^{210}\text{Pb}$  activity and porosity as a function of depth.  $^{210}\text{Pb}$  activities represented by solid boxes were used in determining best-fit parameter values. Samples with no unsupported  $^{210}\text{Pb}$  activity (total activity at background) fall along the ordinate axis. Porosity values are given by circles. The horizontal dashed line marks the boundary between the bioturbated layer and the region below.



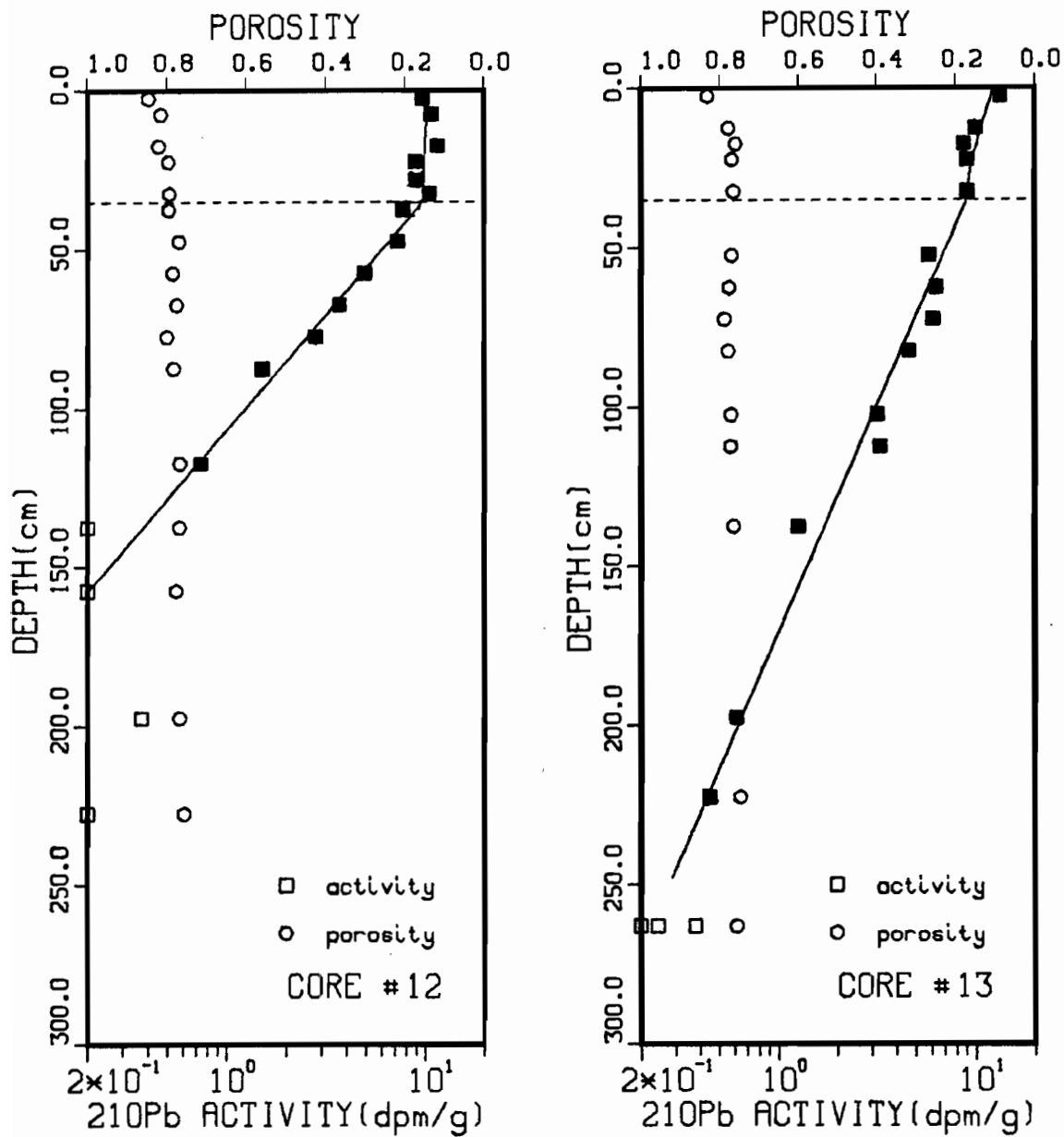


Fig. 2g.--Profiles of unsupported <sup>210</sup>Pb activity and porosity as a function of depth. <sup>210</sup>Pb activities represented by solid boxes were used in determining best-fit parameter values. Samples with no unsupported <sup>210</sup>Pb activity (total activity at background) fall along the ordinate axis. Porosity values are given by circles. The horizontal dashed line marks the boundary between the bioturbated layer and the region below.

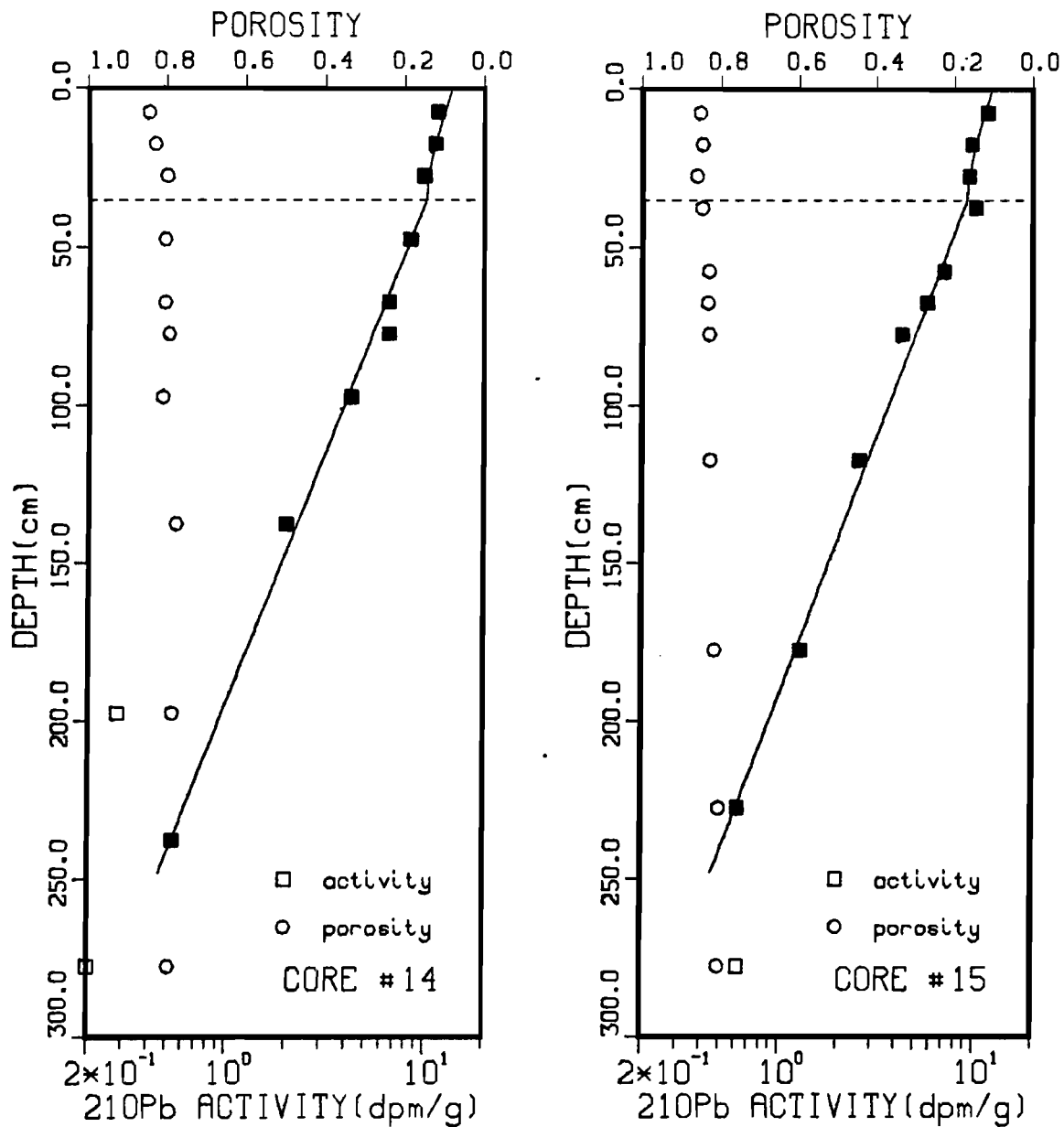


Fig. 2h.--Profiles of unsupported  $^{210}\text{Pb}$  activity and porosity as a function of depth.  $^{210}\text{Pb}$  activities represented by solid boxes were used in determining best-fit parameter values. Samples with no unsupported  $^{210}\text{Pb}$  activity (total activity at background) fall along the ordinate axis. Porosity values are given by circles. The horizontal dashed line marks the boundary between the bioturbated layer and the region below.

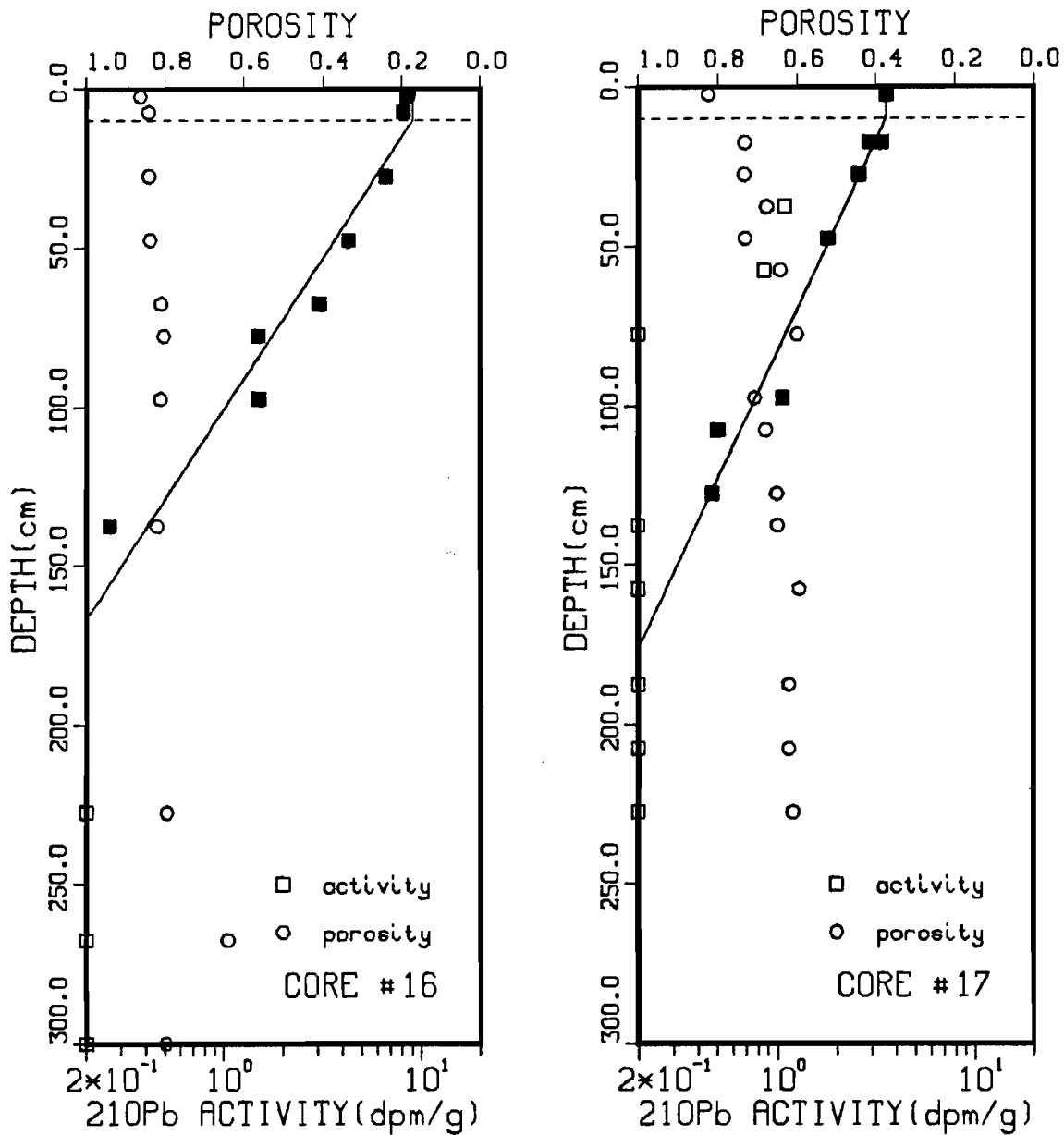


Fig. 2i.--Profiles of unsupported <sup>210</sup>Pb activity and porosity as a function of depth. <sup>210</sup>Pb activities represented by solid boxes were used in determining best-fit parameter values. Samples with no unsupported <sup>210</sup>Pb activity (total activity at background) fall along the ordinate axis. Porosity values are given by circles. The horizontal dashed line marks the boundary between the bioturbated layer and the region below.

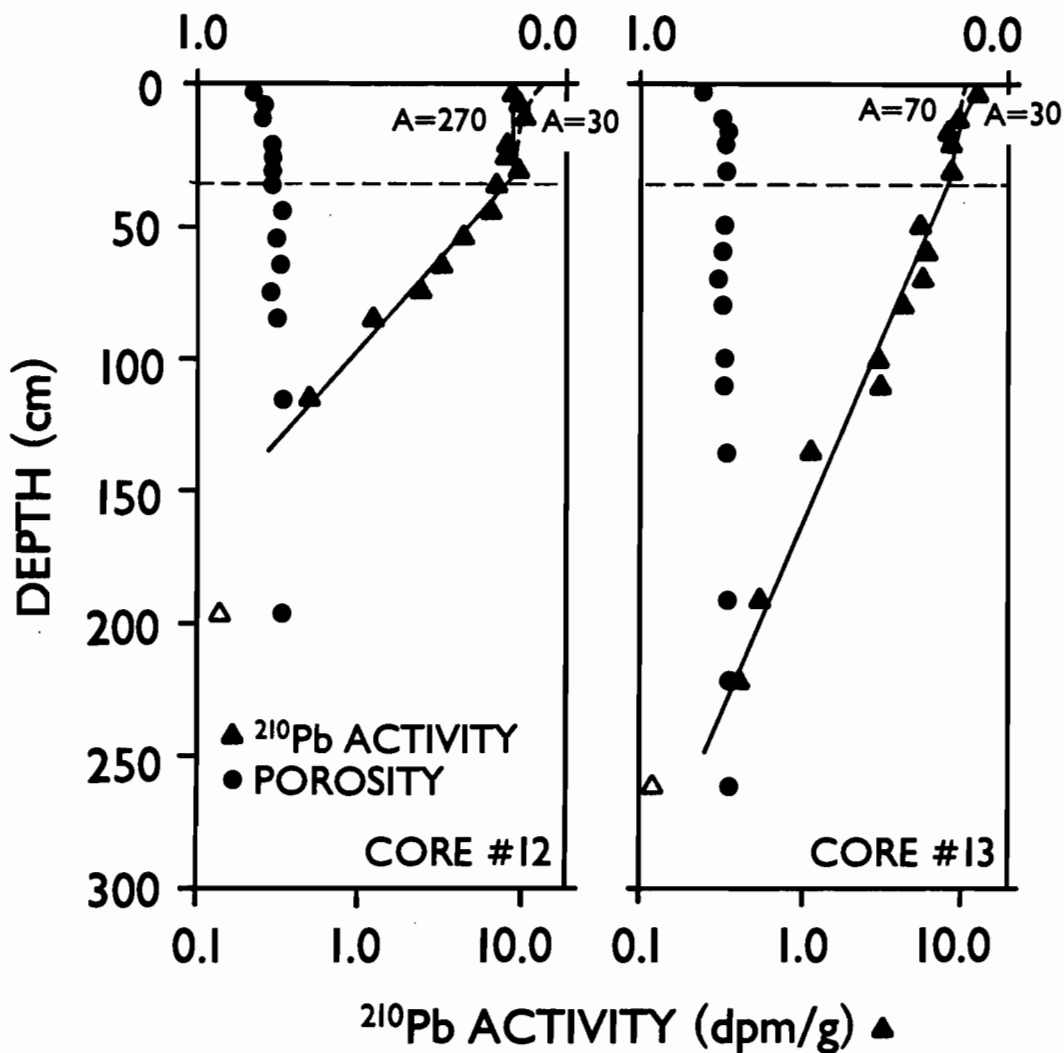


Fig. 3.--Profiles of Cores #12 and 13 with best fit curves for several different values of upper-layer biodiffusivity ( $A_1$ ) in  $\text{cm}^2/\text{yr}$ . Dashed lined marks the boundary between the bioturbated layer and the region below. Open symbols represent data not included in the analysis. The scale of porosity is on the top and reads right to left.

activity down the length of the core. Variability of  $r$  over horizontal distances of tens of meters can be judged from Cores #3, 4, 5 which were taken in succession at a common position relative to a bottom tethered station marker. Two of these rates are consistent though the third has a rate 30% larger; bioturbation depths of the two rate-similar stations are 35 and 40 cm, while the third had a bioturbation depth half that value (Table 1). Cores #7 and 14, nominally taken at the same site but in different years, have values of 0.78 and 1.15 gm/cm<sup>2</sup>/yr.

Comparison of rates from our cores to those of nearby cores of Carpenter *et al.* (1985) generally show similarity in magnitude, though a distinct exception is found near Core #8 where nearby rates are 0.13 and 0.69 gm/cm<sup>2</sup>/yr. The lower of the two rates (Carpenter *et al.* (1985)) is at a station of greater depth (>246 m) than our station (229 m), and the large difference in rates probably reflects real lateral rate differences. This rate variability was also reflected in our attempt to sample the bottom within a topographic depression about 1 km south of Core #13 that resulted in partial penetration of the bottom, indicating a zone of small deposition or even erosion. Small-scale cross-axis changes in sedimentation are also argued from stable Pb profiles (E. Crecelius, unpublished data) from several across-channel transects in the Main Basin. Those consistently show more than a two-fold decrease in the sedimentation rate away from the axis of the channel over distances of slightly more than 1 km.

In light of this accumulation rate variability, one must be wary of drawing too firmly specific conclusions from these data though some general conclusions seem possible. Accumulation rates *en toto* appear to be largest in the central areas near Elliott Bay (Seattle), much lower to the north near Admiralty Inlet, and somewhat smaller to the south through East Passage. The declining sedimentation rates to the north coincide with a coarsening of the bottom sediment, a result from the effect of strong bottom currents there (Baker, 1984). The relatively high deposition region off Elliott Bay and slightly to the north have heretofore gone unmeasured, as have the relatively lower deposition rates in East Passage (Cores #1 and 2). These new data change the overall view that highest accumulation occurs between Seattle and Tacoma (Carpenter *et al.*, 1985) to one where highest accumulation occurs off of and to the north and south of Elliott Bay and perhaps in the vicinity of Commencement Bay (Tacoma).

The sources of sediment for deposition in the Main Basin are possibly three: 1) rivers 2) bluff erosion along the shoreline 3) submarine erosion and slumping of the sidewalls of the Basin (slopes of 20% are common). Atmospheric, biological, and wastewater particulate inputs are small (Carpenter *et al.*, 1985). Little can be said about submarine erosion and slumping because no observations have been made to document its occurrence or importance.

Riverine inputs are based on sparse upriver sediment flux measurements for some rivers and on extrapolations based on gauged flow for the rest (Dexter *et al.*, 1981; Downing, 1983). For example, the sediment yield of the Duwamish is based on daily measurements of vertically integrated sediment flux over a three year period (1963-66) at Tukwila, Washington (U.S. Geological Survey, 1964-66; Santos and Stoner, 1972). Those yields are overestimates of sediment available to the Main Basin, however, because many river-borne

particulates are trapped in the lower rivers and deltas, e.g. dredging records suggest that 87% of the sediment load of the Duwamish is deposited in the lower, navigable section of the river (Harper-Owes, 1983). For the special case of the Duwamish, those sediments have been quasi-annually dredged and redeposited in outer Elliott Bay via dumping; that those sediments are not uniformly spread over the Main Basin is evidenced in contaminant patterns that have been measured at and around the Four Mile Rock dump site (Romberg et al., 1984).

The sediment flux estimates for the Duwamish and Puyallup, rivers that debouch directly into embayments of the Main Basin, are  $1.7 \times 10^{11}$  and  $5.3 \times 10^{11}$  g/yr (Downing, 1983). The Skagit, Stillaquamish, and the Snohomish Rivers together have sediment fluxes of 2-3 times the combined amount of the Duwamish and Puyallup (Downing, 1983), but they discharge into the Whidbey Basin of Puget Sound and whether a significant amount of that material finds its way into the Main Basin is yet unknown. Carpenter et al. (1985) use the sum of flux estimates for most of the principal rivers entering the Sound in arguing that riverine sources alone provide sufficient sediment for a mass balance of supply and  $^{210}\text{Pb}$  measured deposition. Using the entire upriver fluxes of only the Duwamish and Puyallup rivers and distributing that over the area of muds and sandy muds ( $2.6 \times 10^{12}$  cm<sup>2</sup>; Barrick (1982) from the data of Roberts (1979)) leads to an areal average deposition rate of 0.27 gm/cm<sup>2</sup>/yr for the deep Main Basin.

Bluff erosion caused by wave undercutting, ground water seepage, or earthquakes, may also be a significant sediment source. Approximately 135 km of the shoreline around the Main Basin are unstable (Washington State Department of Ecology, 1977-1979). The record of location, frequency of occurrence, and volume of sediment released in bluff erosional events is fragmentary. Tubbs (1974) mapped locations of earthslides that occurred in early 1972 for a 7.5' latitudinal section of the Sound encompassing most of Vashon Island and the shoreline of the Sound to the east. Though the slide locations are only graphically represented, approximately 14 slides likely contributed sediment to the Main Basin during an unusually wet winter and spring. Downing (1983) also noted a 1949 earthquake that caused an earthslide of over  $7.6 \times 10^5$  m<sup>3</sup> in the Tacoma Narrows.

Rates of erosion are uncertain, though Keuler (1979) found rates ranging from 1-12 cm/yr for Skagit County in the north Sound with an average of 7.6 cm/yr; Foster (1976) according to Keuler (1979) reported rates of 8 to 30 cm/yr for the Saanich Peninsula, Vancouver Island, British Columbia; and Tubbs et al. (1974) estimated the upper bluffs at Discovery Park, Seattle, were receding at rates of 15-45 cm/yr over a 20 yr period. Bluff heights around the Sound range from 15 to 150 m; Keuler (1979) also examined the particle size composition of unstable bluffs in Skagit County and found them to contain approximately 70% silts and clays. If unstable bluffs around the Main Basin were receding at an average rate of 10 cm/yr, a conservative estimate of sediment yield from bluff erosion from the values above would be  $3.8 \times 10^{11}$  g/yr (less than half the value of Dexter et al., 1981), leading to an areal average deposition rate for material originating in bluffs of 0.14 gm/cm<sup>2</sup>/yr.

These two sources, riverine and bluff erosion, together support an areal average deposition rate in the lower end of the range we have measured with

$^{210}\text{Pb}$  (0.26 - 1.20 gm/cm<sup>2</sup>/yr). Because the  $^{210}\text{Pb}$  data are from axial stations and deposition rates are thought to be lower off axis, the true areal average deposition rate for fine sediment in the Main Basin that might ultimately come from more complete  $^{210}\text{Pb}$  measurement coverage could well be expected to have a value closer to the lower end of the range of our measured  $^{210}\text{Pb}$  values. How the average deposition would be partitioned among the possible sources of sediment (rivers, bluff erosion, and submarine erosion and slumping) is unclear because of the numerous uncertainties involved in the supply-side estimates.

The episodic and localized nature of earthquake triggered landslides serves to emphasize the interrupted nature, both in space and time, of all shoreline source of sediments. Those slides caused by wave activity are most likely to occur during the winter months. Those triggered by seepage are most like to occur after the heaviest sustained rains of January through March (Downing, 1983). River sources of sediment also have seasonal and interannual variability. River runoff in the Duwamish and Puyallup is highest in December from rains and in June with snow melt; the sediment yield measured in the Duwamish (Santos and Stoner, 1972) was such that in years with the highest and lowest peak water discharge the sediment flux was twice and only 1/3 the 3-year mean value. Submarine erosion and slumping could also be expected to be localized and episodic. Thus, these combined, time and space-variable sources of sediment to the Main Basin ought to lead to a spatially complex and time-variable sedimentation pattern in the Sound. One might expect some reflection of this in short-lived isotopes, e.g. different sedimentation rates at the same location at different times within a year or in different years. That the  $^{210}\text{Pb}$  profiles presented here are generally consistent with an assumption of constant sedimentation must be partly the result of the homogenization of core sections and partly the result of the efficiency of the mixing process underway in the sediment column and along the Sound.

#### 4. CONCLUSIONS

Deposition rates of sediments in the Main Basin of Puget Sound can be as high as 1.20 gm/cm<sup>2</sup>/yr based on accumulations over the past approximately 70 years in cores. These measurements show highest deposition rates occurring in the central region of the Basin off of and north and south of Elliott Bay. Rates five times lower were observed in lower East Passage. Bioturbated layer depths can apparently be as large as 35-40 cm; a core shorter than two or three times that length in some cases may not be adequate to evaluate the sedimentation rate. Bioturbation mixing rates, though poorly determined, appear to be greater than a few tens of cm<sup>2</sup>/yr.

Mass balance calculations point out the need for better resolution of deposition patterns and more accurate characterization of source volumes. The first requires cross-axis and other small-scale variability to be further examined. The second requires a number of issues to be addressed: the role of submarine erosion and slumping; sediment flux to the Main Basin from Whidbey Basin; trapping of riverine sediment by the lower rivers and embayments; the volume, frequencies, and locations of shoreline bluff erosion. The present-day horizon will be deep in sediment cores before these issues are fully resolved.

## 5. ACKNOWLEDGMENTS

We thank R. Carpenter and many colleagues at the Pacific Marine Environmental Laboratory for their constructive comments.

The work has been supported by NOAA Environmental Research Laboratories and by the NOAA Office of Oceanography and Marine Services under the Long Range Effects Research Program/Sec. 202.



## 6. REFERENCES

- Aller, R.C., L.K. Benninger, and J.K. Cochran, 1980. Tracking particle associated processes in nearshore environments by use of  $^{234}\text{Th}/^{238}\text{U}$  disequilibrium. Earth Planet. Sci. Lett., 47, 161-175.
- Baker, E.T., 1984. Patterns of suspended particle distribution and transport in a large fjord-like estuary, J. Geophys. Res., 89(C4), 6553-6566.
- Barrick, R.C., 1982. Flux of aliphatic and polycyclic aromatic hydrocarbons to central Puget Sound from Seattle (Westpoint) primary sewage effluent. Environ. Sci. Technol., 16(10), 682-692.
- Berner, R.A., 1980. Early diagenesis, a theoretical approach. Princeton University Press, Princeton, 241 pp.
- Blank, H.R., Jr., 1950. Rate of sedimentation in the Skagit Bay Region by radium analysis. M.S. Thesis, University of Washington, 28 pp.
- Carpenter, R., M.L. Peterson, and J.T. Bennett, 1982.  $^{210}\text{Pb}$ -derived sediment accumulation and mixing rates for the Washington Continental Slope, Marine Geology, 48, 135-164.
- Carpenter, R., M.L. Peterson, and J.T. Bennett, 1985.  $^{210}\text{Pb}$  derived sediment accumulation and mixing rates for the Greater Puget Sound Region, Marine Geology, in press.
- Christensen, E.R., 1982. A model for radionuclides in sediments influenced by mixing and compaction, J. Geophys. Res., 87, 566-572.
- Collias, E.E., N. McGary, and C.A. Barnes, 1974. Atlas of physical and chemical properties of Puget Sound and its approaches. University of Washington Press, Seattle, WA.
- Dexter, R.N., D.E. Anderson, E.A. Quilan, L.S. Goldstein, R.M. Strickland, S.P. Pavlou, J.R. Clayton, Jr., R.M. Kocan, and M. Landolt, 1981. A summary of knowledge of Puget Sound related to chemical contaminants. NOAA Technical Memorandum OMPA-13, NOAA, Boulder, Co. 435 pp.
- Downing, J.P., 1983. The coast of Puget Sound, its processes and development. Puget Sound Books, a Washington State Sea Grant Publication, University of Washington Press, Seattle, 126 pp.
- Foster, H.D., 1976. Coastal erosion: a natural hazard of the Saanich Peninsula, Vancouver Island. In H.D. Foster (ed)., Victoria: Physical Environment and Development, Victoria, B.C., University of Victoria, Dept. of Geography, Western Geophysical Series, 12, 131-184.
- Gill, A.E., 1982. Atmosphere-Ocean Dynamics. Academic Press, New York.
- Goldberg, E.D. and M. Koide, 1962. Geochronological studies of deep sea sediments by the Io/Th method, Geochim. Cosmochim. Acta, 26, 417-450.
- Guinasso, N.L. and D.R. Shink, 1975. Quantitative estimates of biological mixing in abyssal sediments. J. Geophys. Res., 80, 3032-3034.

- Harper-Owes, 1983. Water quality assessment of the Duwamish estuary, Washington. Report prepared for Municipality of Metropolitan Seattle (METRO), Seattle, WA, 194 pp + appendices.
- Jenkins, G.M. and D.G. Watts, 1968. Spectral analysis and its applications. Holden-Day, San Francisco, 525 pp.
- Keuler, R.F., 1979. Coastal zone processes and geomorphology of Skagit County, Washington. M.S. Thesis. Western Washington University, Bellingham, WA. 127 pp.
- Lavelle, J.W., H.O. Mofjeld, and E.T. Baker, 1984. An in-situ erosion rate for a fine-grained marine sediment. J. Geophys. Res., 89(C4), 6543-6552.
- Lebel, J., N. Silverberg, and G. Sundby, 1982. Gravity core shortening and pore water chemical gradients. Deep Sea Research, 29(11A), 1365-1372.
- Link, J.M., 1982. A biochemical study of Pb-210 in Puget Sound. M.S. Thesis, University of Washington, Seattle, 243 pp.
- Peng, T.H., W.S. Broeker, and W.H. Berger, 1979. Rates of benthic mixing in deep-sea sediment as determined by radioactive tracers. Quaternary Res., 11, 141-149.
- Robbins, J.A., 1978. Geochemical and geophysical application of radioactive lead. In: J.O. Nriagu (ed)., The Biogeochemistry of Lead in the Environment. Elsevier, Amsterdam, 285-393.
- Robbins, J.A., and D.N. Edgington, 1975. Determination of recent sedimentation rates in Lake Michigan using Pb-210 and Cs-137., Geochim. Cosmochim. Acta, 39, 285-304.
- Roberts, R.W., 1979. Sediment distribution maps for Puget Sound. Unpublished. University of Washington, Seattle.
- Romberg, G.P., S.P. Pavlou, R.F. Shokes, W. Hom, E.A. Crecelius, P. Hamilton, J.T. Gunn, R.D. Muench, and J. Vinelli, 1984. Toxicant pretreatment planning study, technical report C1: presence, distribution and fate of toxicants in Puget Sound and Lake Washington, Municipality of Metropolitan Seattle (METRO), Seattle, WA.
- Santos, J.F. and J.D. Stoner, 1972. Physical, chemical, and biological aspects of the Duwamish River Estuary, King County, Washington 1963-67. U.S. Geol. Survey Water Supply Paper 1873-C, Washington, D.C., 74 pp.
- Schell, W.R., 1974. Sedimentation rates and mean residence time of stable Pb and Pb-210 in Lake Washington, Puget Sound estuaries and a coastal region. University of Washington, College of Fisheries, Ecology Lab., Seattle, Wash., USAEC Rep. RLO-2225-T14-6.
- Schell, W.R., and A. Nevissi, 1977. Heavy metals from waste disposed in central Puget Sound. Environ. Sci. Technol., 11(9), 887-893.

- Schell, W.R., A. Nevissi, D. Piper, G. Christian, J. Murray, D. Spyradakis, S. Olsen, D. Huntaner, E. Knudson, D. Zafiropoulos, 1977. Heavy metals near the West Point outfall and in the Central Basin of Puget Sound, Municipality of Metropolitan Seattle (METRO), Seattle, WA, 174 pp.
- Tubbs, D., 1974. Landslides and associated damage during early 1972 in part of West-central King County, Washington. Miscellaneous Investigation Series Map #I-852-B. U.S. Geological Survey, Washington, D.C.
- Tubbs, D., T. Dunne, and R. Sternberg, 1974. Discovery Park inventory and natural history report (Earth Services component). Institute for Environmental Studies Rept., University of Washington, Seattle, WA, p. 15-46.
- U.S. Geological Survey, 1964-1966. Quality of the surface waters of the United States. Geological Survey Water Supply Papers 1959, 1966 and 1996. U.S. Government Printing Office, Washington, D.C.
- Washington State Department of Ecology, 1977-1979. The coastal zone atlas of Washington, v. 1-12. State of Washington, Olympia, WA.

## Appendix I: Salt Correction Calculations

Any sampled volume within a core contains water, salt, and sediment. If one is to calculate deposition rates of sediment alone, one must be able to calculate the contribution of occluded salt to the measured dry mass before calculating porosities and radioisotope activity per salt-free unit mass. Typically, the dry weight fraction (D) of each core section is measured. If in addition the salinity of the occluded seawater (S), its density ( $\rho$ ), and the dry density of sediment were known, then the porosity, wet density, and fraction of dry weight due to sediment alone (salt excluded) could be calculated in the following way:

Let the volume fractions and densities of water, salt and sediment in a unit volume of core material be  $V_w$ ,  $V_n$ ,  $V_s$  and  $\rho_w$ ,  $\rho_n$ ,  $\rho_s$  respectively. For the unit volume ( $V_w + V_n + V_s = 1$ ), the following definitions obtain:

density of seawater: 
$$\rho = \frac{\rho_n V_n + \rho_w V_w}{V_n + V_w}$$

salinity: 
$$S = \frac{\rho_n V_n}{\rho_n V_n + \rho_w V_w}$$

dry weight fraction: 
$$D = \frac{\rho_n V_n + \rho_s V_s}{\rho_w V_w + \rho_n V_n + \rho_s V_s}$$

These equations can be rewritten as three simultaneous equations for the three unknown weight fractions of each component:  $\rho_w V_w$ ,  $\rho_n V_n$ ,  $\rho_s V_s$ . The quantities presumed known or measured are:  $\rho(S, T)$ ,  $\rho_s$ , S, and D, where  $\rho$ , the density of seawater, is a function of salinity and temperature.

The three simultaneous equations, when solved, allow the following quantities to be derived:

wet density: 
$$W \equiv \frac{\rho_w V_w + \rho_n V_n + \rho_s V_s}{V_w + V_n + V_s}$$

$$= \frac{\rho_s \rho (1-S)}{[\rho_s (1-D) + \rho (D-S)]}$$

porosity: 
$$\phi \equiv \frac{V_w + V_n}{V_w + V_s + V_n}$$

$$= \frac{\rho_s (1-D)}{[\rho_s (1-D) + \rho (D-S)]}$$

weight corrector:

$$F_c \equiv \frac{\rho_s V_s}{\rho_n V_n + \rho_s V_s}$$
$$= \frac{(D-S)}{[D(1-S)]}$$

The measured dry weight D can be multiplied by  $F_c$  to get the salt-free dry weight of sediment for normalization of activity measurements. The porosity must also be calculated before mass accumulation rate calculations can be made.

In the present context, values of temperature of 11°C and a salinity of 30‰, corresponding to typical bottom water conditions in Puget Sound (Collias et al., 1974), were used in the equation of state (Gill, 1982) to derive a value of  $\rho = 1.0229 \text{ g/cm}^3$ . Sediment density, as measured on representative samples, was  $2.6 \text{ g/cm}^3$  and the salinity fraction was  $S = 0.030$ . Salt-free porosity and  $^{210}\text{Pb}$  activity per unit mass of salt-free sediment were calculated for each core section using these values and the measured dry weight (Appendix II).

**Appendix II: Data Tables**

CORE-1

DATE: March 1984

LAT: 47°21.9' N

LONG: 122°22.0' W

Depth	Percent Dry Weight	Total $^{210}\text{Pb}$ Activity (dpm/g, salt-free)	Porosity	Unsupported $^{210}\text{Pb}$ (dpm/g, salt-free)
0- 2	30.0	9.12±0.28	0.871	8.40
4- 6	33.0	7.54±0.22	0.853	6.82
9- 11	35.3	7.50±0.34	0.839	6.78
14- 16	36.0	7.68±0.23	0.835	6.96
19- 21	33.1	6.01±0.23	0.853	5.29
29- 31	33.6	4.80±0.25	0.877	4.08
37- 41	35.1	4.19±0.17	0.840	3.47
49- 51	37.4	2.03±0.15	0.826	1.31
59- 61	35.8	2.02±0.14	0.836	1.30
69- 71	36.3	1.52±0.09	0.833	0.80
79- 81	36.0	1.06±0.07	0.835	0.34
89- 91	36.6	0.77±0.09	0.831	-
99-101	35.6	0.85±0.07	0.837	-
119-121	38.8	0.66±0.06	0.817	-
139-141	37.9	0.64±0.05	0.823	-
159-161	38.6	0.62±0.06	0.818	-
179-181	36.7	0.75±0.08	0.830	-
199-201	35.7	0.71±0.08	0.837	-
219-221	40.2	0.70±0.06	0.807	-
259-261	38.6	0.86±0.09	0.818	-

CORE-2

DATE: March 1984

LAT: 47°23.8' N

LONG: 122°21.2' W

Depth	Percent Dry Weight	Total <sup>210</sup> Pb Activity (dpm/g, salt-free)	Porosity	Unsupported <sup>210</sup> Pb (dpm/g, salt-free)
0- 2	30.0	9.90±0.28	0.871	9.18
4- 6	33.5	8.30±0.27	0.850	7.58
9- 11	34.4	8.75±0.32	0.845	8.03
14- 16	32.5	7.60±0.22	0.856	6.88
19- 21	34.9	7.32±0.28	0.842	6.60
29- 31	32.9	7.53±0.32	0.853	6.81
39- 41	36.0	5.15±0.16	0.835	4.43
49- 51	35.3	4.09±0.19	0.839	3.37
59- 61	41.4	1.53±0.13	0.799	0.81
69- 71	40.7	1.47±0.12	0.804	0.75
79- 81	38.4	0.99±0.09	0.819	0.27
89- 91	38.7	0.95±0.09	0.817	0.23
99-101	39.9	0.86±0.09	0.809	-
119-121	38.2	0.68±0.06	0.821	-
139-141	37.9	0.67±0.08	0.823	-
159-161	39.1	0.89±0.07	0.815	-
179-181	41.6	0.65±0.08	0.761	-
199-201	40.9	0.57±0.08	0.802	-
219-221	41.6	0.89±0.09	0.798	-
259-261	43.2	0.57±0.08	0.786	-



CORE-3

DATE: March 1984

LAT: 47°25.6' N

LONG: 122°23.5' W

Depth	Percent Dry Weight	Total <sup>210</sup> Pb Activity (dpm/g, salt-free)	Porosity	Unsupported <sup>210</sup> Pb (dpm/g, salt-free)
0- 2	31.2	9.57±0.28	0.864	8.63
4- 6	33.8	9.60±0.30	0.848	8.66
9- 11	35.5	9.89±0.28	0.838	8.95
14- 16	31.8	9.21±0.33	0.860	8.27
19- 21	31.6	9.87±0.32	0.862	8.93
29- 31	33.3	8.25±0.26	0.852	7.31
39- 41	36.7	8.58±0.26	0.830	7.64
49- 51	32.7	7.05±0.24	0.855	6.11
59- 61	36.0	5.64±0.21	0.835	4.70
69- 71	35.7	5.04±0.19	0.837	4.10
79- 81	38.0	4.74±0.22	0.822	3.80
89- 91	38.0	3.58±0.16	0.822	2.64
99-101	40.6	3.14±0.16	0.805	2.20
119-121	35.9	2.88±0.12	0.835	1.94
139-141	40.1	1.98±0.13	0.808	1.04
159-161	41.0	1.53±0.09	0.802	0.59
179-181	37.8	1.18±0.11	0.823	0.24
199-201	38.4	0.87±0.09	0.819	-
219-221	39.8	1.02±0.07	0.810	-
259-261	39.0	0.94±0.07	0.815	-

CORE-4

DATE: March 1984

LAT: 47°25.6' N

LONG: 122°23.5' W

Depth	Percent Dry Weight	Total $^{210}\text{Pb}$ Activity (dpm/g, salt-free)	Porosity	Unsupported $^{210}\text{Pb}$ (dpm/g, salt-free)
0- 2	29.1	10.61±0.31	0.876	9.64
4- 6	34.1	9.86±0.25	0.847	8.89
9- 11	33.9	11.44±0.34	0.848	10.47
14- 16	33.7	8.85±0.24	0.849	7.88
19- 21	32.2	9.36±0.22	0.858	8.39
29- 31	33.6	8.60±0.28	0.850	7.63
39- 41	35.6	7.31±0.27	0.837	6.34
49- 51	36.0	6.77±0.23	0.835	5.80
59- 61	35.5	5.30±0.22	0.837	4.33
69- 71	37.6	5.09±0.22	0.825	4.12
79- 81	39.9	4.36±0.18	0.809	3.39
89- 91	37.6	4.21±0.17	0.825	3.24
99-101	37.2	4.95±0.21	0.827	3.98
119-121	38.3	2.26±0.12	0.820	1.29
139-141	36.7	2.56±0.17	0.830	1.59
159-161	40.9	1.70±0.11	0.802	0.73
179-181	37.7	1.55±0.11	0.824	0.58
199-201	38.8	0.94±0.07	0.817	-
219-221	39.1	0.98±0.12	0.815	-
259-261	37.6	0.99±0.07	0.825	-

CORE-5

DATE: March 1984

LAT: 47°25.6' N

LONG: 122°23.5' W

Depth	Percent Dry Weight	Total $^{210}\text{Pb}$ Activity (dpm/g, salt-free)	Porosity	Unsupported $^{210}\text{Pb}$ (dpm/g, salt-free)
0- 2	31.4	10.04±0.31	0.863	9.22
4- 6	32.8	9.71±0.32	0.855	8.89
9- 11	31.2	8.64±0.29	0.864	7.82
14- 16	33.5	8.36±0.27	0.850	7.54
19- 21	32.6	7.69±0.29	0.856	6.87
29- 31	35.6	6.10±0.27	0.837	5.28
39- 41	34.6	7.83±0.25	0.843	7.01
49- 51	34.4	6.68±0.21	0.845	5.86
59- 61	35.0	4.83±0.25	0.841	4.01
69- 71	37.4	5.48±0.20	0.826	4.66
79- 81	*	2.98±0.19	*	2.16
89- 91	37.9	3.04±0.12	0.823	2.22
99-101	35.8	3.03±0.14	0.836	2.21
119-121	40.5	1.87±0.13	0.805	1.05
139-141	40.0	1.43±0.11	0.808	0.61
159-161	37.9	1.36±0.11	0.823	0.54
179-181	39.1	1.00±0.10	0.815	0.18
199-201	38.6	1.09±0.10	0.818	0.27
219-221	36.6	0.77±0.10	0.831	-
259-261	37.6	0.86±0.09	0.825	-

CORE-6

DATE: March 1984

LAT: 47°31.6' N

LONG: 122°25.4' W

Depth	Percent Dry Weight	Total <sup>210</sup> Pb Activity (dpm/g, salt-free)	Porosity	Unsupported <sup>210</sup> Pb (dpm/g, salt-free)
0- 2	30.6	11.28±0.42	0.867	10.28
4- 6	35.2	11.76±0.40	0.840	10.76
9- 11	35.5	10.19±0.29	0.838	9.19
14- 16	36.3	9.48±0.27	0.833	8.48
19- 21	35.8	9.86±0.30	0.836	8.86
29- 31	37.2	10.42±0.26	0.827	9.42
39- 41	37.5	8.85±0.27	0.825	7.85
59- 61	37.5	8.11±0.16	0.825	7.11
69- 71	38.1	7.39±0.23	0.821	6.39
79- 81	36.7	7.82±0.35	0.830	6.82
89- 91	36.0	5.89±0.36	0.835	4.89
99-101	39.1	6.17±0.21	0.815	5.17
119-121	38.0	4.97±0.25	0.822	3.97
139-141	40.2	4.29±0.17	0.807	3.29
159-161	39.3	4.53±0.23	0.813	3.53
179-181	41.0	3.28±0.17	0.801	2.28
199-201	40.6	2.74±0.13	0.805	1.74
219-221	41.3	1.85±0.16	0.801	0.85
259-261	42.4	1.27±0.11	0.792	0.27

CORE-7

DATE: March 1984

LAT: 47°36.9' N

LONG: 122°26.75' W

Depth	Percent Dry Weight	Total <sup>210</sup> Pb Activity (dpm/g, salt-free)	Porosity	Unsupported <sup>210</sup> Pb (dpm/g, salt-free)
0- 2	32.3	13.57±0.34	0.857	12.47
4- 6	36.6	11.55±0.32	0.831	10.45
9- 11	37.8	11.00±0.30	0.823	9.90
14- 16	37.6	12.13±0.36	0.825	11.03
19- 21	40.5	9.81±0.28	0.805	8.71
29- 31	36.9	8.53±0.28	0.829	7.43
39- 41	40.9	6.90±0.22	0.802	5.80
49- 51	38.6	4.58±0.29	0.818	3.48
69- 71	38.4	6.52±0.28	0.819	5.42
79- 81	40.1	4.55±0.23	0.808	3.45
89- 91	39.1	3.65±0.23	0.815	2.55
99-101	38.1	3.68±0.23	0.821	2.58
119-121	41.0	2.54±0.17	0.802	1.44
139-141	42.7	1.81±0.14	0.790	0.71
159-161	42.2	1.51±0.17	0.793	0.41
179-181	43.2	1.52±0.13	0.785	0.42
199-201	44.1	1.30±0.13	0.780	0.20
219-221	41.5	1.20±0.09	0.798	-
259-261	43.7	1.18±0.11	0.783	-

## CORE-8

DATE: March 1984

LAT: 47°39.75' N

LONG: 122°27.9' W

Depth	Percent Dry Weight	Total <sup>210</sup> Pb Activity (dpm/g, salt-free)	Porosity	Unsupported <sup>210</sup> Pb (dpm/g, salt-free)
0- 2	36.2	11.09±0.39	0.833	10.22
4- 6	38.2	9.88±0.33	0.821	9.01
9- 11	42.0	10.19±0.27	0.795	9.32
14- 16	42.0	10.93±0.30	0.795	10.06
19- 21	42.3	9.21±0.25	0.793	8.34
29- 31	45.1	8.18±0.39	0.772	7.31
39- 41	41.1	7.28±0.25	0.801	6.41
49- 51	42.6	6.23±0.24	0.790	5.36
59- 61	42.7	6.20±0.27	0.790	5.33
69- 71	39.3	6.84±0.27	0.813	5.97
79- 81	43.8	3.00±0.17	0.782	2.13
89- 91	43.4	3.06±0.24	0.785	2.19
99-101	44.4	2.69±0.17	0.778	1.82
119-121	43.3	1.69±0.14	0.785	0.82
139-141	46.3	1.24±0.12	0.767	0.37
159-161	45.3	1.13±0.12	0.771	0.26
179-181	45.7	0.94±0.10	0.768	-
199-201	47.2	0.99±0.12	0.757	-
219-221	46.3	0.92±0.11	0.763	-
259-261	45.8	0.64±0.09	0.767	-

CORE-9

DATE: August 1982

LAT: 47°26.7' N

LONG: 122°23.55' W

Depth	Percent Dry Weight	Total $^{210}\text{Pb}$ Activity (dpm/g, salt-free)	Porosity	Unsupported $^{210}\text{Pb}$ (dpm/g, salt-free)
4- 6	44.3	6.15±0.22	0.778	5.61
7- 8	45.0	5.48±0.26	0.773	4.94
9- 11	46.4	5.77±0.24	0.763	5.23
14- 16	45.3	4.54±0.24	0.771	4.00
19- 21	47.0	4.15±0.22	0.758	3.61
24- 24	53.2	2.79±0.13	0.707	2.25
29- 31	53.8	1.97±0.13	0.702	1.43
32- 34	52.2	1.85±0.10	0.716	1.31
35- 38	48.4	2.74±0.15	0.747	2.20
39- 41	55.9	1.74±0.11	0.683	1.20
49- 51	54.4	1.36±0.11	0.696	0.82
59- 61	49.9	1.88±0.12	0.735	1.34
69- 71	60.3	0.45±0.06	0.640	-
79- 81	54.6	1.65±0.12	0.695	1.11
89- 91	56.6	1.29±0.11	0.676	0.75
99-101	67.6	0.56±0.08	0.559	-
109-111	66.6	0.54±0.08	0.571	-
119-121	68.2	0.57±0.08	0.552	-
129-131	67.8	0.48±0.08	0.557	-

CORE-10

DATE: March 1984

LAT: 47°58.8' N

LONG: 122°19.5' W

Depth	Percent Dry Weight	Total <sup>210</sup> Pb Activity (dpm/g, salt-free)	Porosity	Unsupported <sup>210</sup> Pb (dpm/g, salt-free)
0- 2	31.8	8.60±0.33	0.860	8.00
4- 6	34.8	8.12±0.35	0.842	7.52
9- 11	37.3	7.14±0.33	0.827	6.54
14- 16	39.1	6.46±0.30	0.815	5.86
19- 21	40.9	4.51±0.23	0.802	3.91
29- 31	39.2	3.92±0.23	0.815	3.32
39- 41	39.6	3.80±0.28	0.811	3.20
49- 51	39.6	2.78±0.15	0.811	2.18
59- 61	38.5	2.75±0.19	0.819	2.15
64- 66	39.8	1.12±0.15	0.810	0.52
69- 71	39.4	1.61±0.13	0.812	1.01
79- 81	40.6	0.93±0.12	0.805	0.33
89- 91	41.4	0.98±0.10	0.799	0.38
99-101	43.1	0.70±0.14	0.787	-
109-111	37.8	2.00±0.16	0.823	-
119-121	42.6	0.68±0.09	0.791	-
139-141	42.3	0.65±0.08	0.793	-
159-161	41.9	0.62±0.08	0.795	-
179-181	42.8	0.34±0.07	0.789	-
184-186	42.3	0.73±0.08	0.793	-



CORE-11

DATE: August 1982

LAT: 47°49.4' N

LONG: 122°25.8' W

Depth	Percent Dry Weight	Total $^{210}\text{Pb}$ Activity (dpm/g, salt-free)	Porosity	Unsupported $^{210}\text{Pb}$ (dpm/g, salt-free)
0- 5	53.5	11.99±0.48	0.701	10.98
5- 10	53.8	11.00±0.44	0.698	9.99
10- 15	58.4	9.69±0.39	0.657	8.68
20- 25	58.9	5.73±0.34	0.652	4.72
35- 40	62.1	4.93±0.35	0.620	3.92
60- 65	60.0	2.37±0.26	0.641	1.36
70- 75	54.9	1.39±0.25	0.689	0.38
80- 85	53.8	1.26±0.33	0.698	0.25
100-105	54.6	1.00±0.30	0.691	-
125-130	56.8	1.72±0.33	0.672	-
175-180	61.9	0.92±0.27	0.622	-
225-230	54.8	1.46±0.25	0.689	-
270-275	54.7	1.13±0.29	0.691	-

CORE-12

DATE: August 1982

LAT: 47°43.0' N

LONG: 122°24.3' W

Depth	Percent Dry Weight	Total <sup>210</sup> Pb Activity (dpm/g, salt-free)	Porosity	Unsupported <sup>210</sup> Pb (dpm/g, salt-free)
0- 5	33.7	10.65±0.37	0.846	9.84
5- 10	38.5	11.70±0.40	0.815	10.89
15- 20	37.6	12.51±0.53	0.821	11.70
20- 25	41.3	9.89±0.36	0.796	9.08
25- 30	41.4	9.62±0.44	0.795	8.81
30- 35	41.6	11.44±0.36	0.794	10.63
35- 40	41.3	8.59±0.38	0.796	7.78
45- 50	45.0	8.15±0.41	0.769	7.34
55- 60	42.9	5.79±0.24	0.785	4.98
65- 70	44.3	4.55±0.28	0.775	3.74
75- 80	40.7	3.63±0.22	0.800	2.82
85- 90	43.2	2.34±0.14	0.783	1.53
115-120	45.5	1.56±0.14	0.766	0.75
135-140	45.3	0.66±0.16	0.767	-
155-160	44.1	0.61±0.13	0.776	-
195-200	45.3	1.18±0.18	0.767	-
225-230	46.7	0.77±0.13	0.756	-

CORE-13

DATE: August 1982

LAT: 47°42.3' N

LONG: 122°26.4' W

Depth	Percent Dry Weight	Total $^{210}\text{Pb}$ Activity (dpm/g, salt-free)	Porosity	Unsupported $^{210}\text{Pb}$ (dpm/g, salt-free)
0- 5	36.2	14.46±0.70	0.830	13.46
10- 15	43.9	11.09±0.45	0.777	10.09
15- 20	46.4	9.79±0.46	0.759	8.79
20- 25	45.1	10.11±0.55	0.769	9.11
30- 35	45.6	10.13±0.65	0.765	9.13
50- 55	45.0	6.85±0.37	0.769	5.85
60- 65	44.2	7.35±0.50	0.775	6.35
70- 75	42.6	7.13±0.28	0.787	6.13
80- 85	43.9	5.64±0.27	0.777	4.64
100-105	44.9	4.23±0.22	0.770	3.23
110-115	44.8	4.33±0.29	0.771	3.33
135-140	45.9	2.27±0.42	0.763	1.27
195-200	46.5	1.62±0.41	0.758	0.62
220-225	47.9	1.45±0.36	0.747	0.45
260-264	46.7	0.87±0.18	0.756	-
260-264	*	1.38±0.30	*	-
260-264	*	1.24±0.19	*	-

CORE-14

DATE: August 1982

LAT: 47°36.9' N

LONG: 122°26.8' W

Depth	Percent Dry Weight	Total $^{210}\text{Pb}$ Activity (dpm/g, salt-free)	Porosity	Unsupported $^{210}\text{Pb}$ (dpm/g, salt-free)
5- 10	33.5	12.65±0.51	0.847	11.65
15- 20	36.1	12.35±0.49	0.831	11.35
25- 30	40.6	10.95±0.33	0.801	9.95
45- 50	39.8	9.47±0.38	0.806	8.47
65- 70	39.8	7.60±0.61	0.806	6.60
75- 80	41.5	7.62±0.61	0.795	6.62
95-100	39.2	5.28±0.74	0.811	4.28
135-140	44.2	3.02±0.33	0.775	2.02
195-200	42.8	1.28±0.40	0.785	0.28
235-240	43.4	1.54±0.32	0.781	0.54
275-280	41.8	0.94±0.36	0.793	-

CORE-15

DATE: August 1982

LAT: 47°28.8' N

LONG: 122°24.4' W

Depth	Percent Dry Weight	Total <sup>210</sup> Pb Activity (dpm/g, salt-free)	Porosity	Unsupported <sup>210</sup> Pb (dpm/g, salt-free)
5- 10	32.7	12.74±0.38	0.852	11.74
15- 20	33.6	10.72±0.32	0.847	9.72
25- 30	31.3	10.45±0.31	0.861	9.45
35- 40	33.4	11.20±0.45	0.848	10.20
55- 60	36.3	8.05±0.32	0.830	7.05
65- 70	35.9	6.76±0.34	0.832	5.76
75- 80	36.4	5.32±0.32	0.829	4.32
115-120	36.9	3.61±0.32	0.826	2.61
175-180	38.8	2.30±0.30	0.813	1.30
225-230	40.5	1.62±0.24	0.802	0.62
275-280	40.3	1.62±0.24	0.803	0.62

CORE-16

DATE: August 1982

LAT: 47°21.0' N

LONG: 122°24.4' W

Depth	Percent Dry Weight	Total <sup>210</sup> Pb Activity (dpm/g, salt-free)	Porosity	Unsupported <sup>210</sup> Pb (dpm/g, salt-free)
0- 5	31.0	9.89±0.40	0.863	8.55
5- 10	34.3	9.50±0.38	0.842	8.16
25- 30	34.3	8.00±0.48	0.842	6.66
45- 50	34.8	5.64±0.34	0.839	4.30
65- 70	39.1	4.38±0.35	0.811	3.04
75- 80	40.1	2.84±0.31	0.804	1.50
95-100	39.0	2.85±0.60	0.812	1.51
135-140	37.7	1.60±0.27	0.821	0.26
225-230	41.4	1.31±0.22	0.795	-
265-270	60.3	1.49±0.22	0.638	-
300-305	41.2	1.25±0.30	0.797	-

CORE-17

DATE: August 1982

LAT: 47°18.7' N

LONG: 122°27.7' W

Depth	Percent Dry Weight	Total <sup>210</sup> Pb Activity (dpm/g, salt-free)	Porosity	Unsupported <sup>210</sup> Pb (dpm/g, salt-free)
0- 5	37.3	4.21±0.23	0.823	3.59
15- 20	49.8	4.02±0.13	0.732	3.40
15- 20	*	3.55±0.13	0.732	2.93
25- 30	49.7	3.21±0.16	0.733	2.59
35- 40	56.2	1.71±0.13	0.677	1.09
45- 50	49.9	2.42±0.60	0.731	1.80
55- 60	59.8	1.48±0.20	0.643	0.86
75- 80	64.0	0.68±0.06	0.600	-
95-100	52.8	1.69±0.10	0.706	1.07
105-110	56.0	1.13±0.13	0.679	0.51
125-130	59.0	1.09±0.13	0.651	0.47
135-140	59.2	0.56±0.09	0.649	-
155-160	64.5	0.71±0.07	0.595	-
185-190	62.0	0.72±0.22	0.621	-
205-210	62.0	0.57±0.10	0.621	-
225-230	63.1	0.53±0.10	0.610	-